

Enhanced effects of variation of the fundamental constants in laser interferometers and application to dark matter detection

Y. V. Stadnik^{1*} and V. V. Flambaum^{1,2}

¹ *School of Physics, University of New South Wales, Sydney 2052, Australia and*

² *Mainz Institute for Theoretical Physics, Johannes Gutenberg University Mainz, D 55122 Mainz, Germany*

(Dated: July 16, 2022)

We outline new laser interferometer measurements to search for variation of the electromagnetic fine-structure constant α and particle masses (including a non-zero photon mass). We propose a strontium optical lattice clock – silicon single-crystal cavity interferometer as a novel small-scale platform for these new measurements. Multiple passages of a light beam inside an interferometer enhance the effects due to variation of the fundamental constants by the mean number of passages ($N_{\text{eff}} \sim 10^2$ for a large-scale gravitational-wave detector, such as LIGO, Virgo, GEO600 or TAMA300, while $N_{\text{eff}} \sim 10^5$ for a strontium clock – silicon cavity interferometer). Our proposed laser interferometer measurements may be implemented as an extremely precise tool in the direct detection of scalar dark matter that forms an oscillating classical field or topological defects.

PACS numbers: 07.60.Ly,95.35.+d,06.20.Jr,06.30.Ft

Introduction. — Dark matter remains one of the most important unsolved problems in contemporary physics. Astronomical observations indicate that the energy density of dark matter exceeds that of ordinary matter by a factor of five [1]. Extensive laboratory searches for weakly interacting massive particle (WIMP) dark matter through scattering-off-nuclei experiments have failed to produce a strong positive result to date, see e.g. Refs. [2–7], which has spurred significant interest of late in searching for alternate well-motivated forms of dark matter, such as ultralight (sub-eV mass) spin-0 particles that form either an oscillating classical field or topological defects, see e.g. Refs. [8–28].

The idea that the fundamental constants of Nature might vary with time can be traced as far back as the large numbers hypothesis of Dirac, who hypothesised that the gravitational constant G might be proportional to the reciprocal of the age of the Universe [29]. More contemporary theories, which predict a variation of the fundamental constants on cosmological timescales, typically invoke a (nearly) massless underlying dark energy-type field, see e.g. the review [30] and the references therein. Most recently, a new model for the cosmological evolution of the fundamental constants of Nature has been proposed in Ref. [28], in which the interaction of an oscillating classical scalar dark matter field with ordinary matter via quadratic interactions produces both ‘slow’ linear-in-time drifts and oscillating-in-time variations of the fundamental constants [31]. Topological defects, which are stable, extended-in-space forms of dark matter that consist of light scalar dark matter fields stabilised by a self-interaction potential [35] and which interact with ordinary matter, produce transient-in-time variations of the fundamental constants [20, 21].

The oscillating-in-time and transient-in-time variations of the fundamental constants produced by scalar dark matter can be sought for in the laboratory using high-precision measurements, which include atomic clocks [36–43], highly-charged ions [44–49], molecules [50–55] and nuclear clocks [56–62], in which two transition frequencies are compared over time.

Instead of comparing two transition frequencies over time, we may instead compare a photon wavelength with an interferometer arm length, in order to search for variations of the fundamental constants [24, 63, 64] (see also [65, 66] for some other applications). In the present work, we outline new laser interferometer measurements to search for variation of the electromagnetic fine-structure constant and particle masses (including a non-zero photon mass). We propose a strontium optical lattice clock – silicon single-crystal cavity interferometer as a novel small-scale platform for these new measurements. The existing small-scale hydrogen maser – cryogenic sapphire oscillator system [64] and existing large-scale gravitational wave detectors, such as LIGO [67], Virgo [68], GEO600 [69], TAMA300 [70], eLISA [71] or the Fermilab Holometer [72], can also be used as platforms for some of our newly proposed measurements. We demonstrate that multiple passages of a light beam inside an interferometer enhance the effects due to variation of the fundamental constants by the mean number of passages.

General Theory. — Unless explicitly indicated otherwise, we employ the natural units $\hbar = c = 1$ in the present work. Alterations in the electromagnetic fine-structure constant $\alpha = e^2/\hbar c$, where $-e$ is the electron charge, $\hbar = h/2\pi$ is the reduced Planck constant and c is the photon speed, or particle masses (including a non-zero photon mass m_γ) produce alterations in the accumulated phase of the light beam inside an interferometer $\Phi = \omega L/c$, since an atomic transition frequency ω and

* y.stadnik@unsw.edu.au

length of a solid $L \sim Na_B$, where N is the number of atoms and $a_B = \hbar^2/m_e e^2$ is the Bohr radius (m_e is the electron mass), both depend on the fundamental constants and particle masses. Alterations in the accumulated phase can be expressed in terms of the sensitivity coefficients K_X , which are defined by:

$$\frac{\delta\Phi}{\Phi} = \sum_{X_i=\alpha, m_e, \dots} K_{X_i} \frac{\delta X_i}{X_i} + K_{m_\gamma} \left(\frac{m_\gamma}{m_e}\right)^2, \quad (1)$$

where the sum runs over all relevant fundamental constants $X_i = \alpha, m_e, \dots$ (except photon mass). The sensitivity coefficients depend on the specific measurement that is performed. In order to define the variation of dimensionful parameters, such as m_e , we assume that such variations are due to the interactions of dark matter with ordinary matter, see e.g. Ref. [28]. The sensitivity coefficients, which we derive below, are for single-arm interferometers, but are readily carried over to the case of two-arm interferometers, for which the observable quantity is the phase difference $\Delta\Phi = \Phi_1 - \Phi_2$ between the two arms.

Multiple reflections enhance observable effects due to variation of the fundamental constants by the effective mean number of passages N_{eff} . This is seen as follows. For multiple reflections of a continuous light source that forms a standing wave (in the absence of variation of the fundamental constants), we sum over all possible number of reflections n :

$$\sum_{n=1}^{\infty} \exp[-n(\kappa - i\Phi)] = \frac{1}{\exp(\kappa - i\Phi) - 1}, \quad (2)$$

where $\kappa \equiv 1/N_{\text{eff}}$ is the attenuation factor that accounts for the loss of light amplitude after a single to-and-back passage along the length of the arm, and $\Phi = 2\pi m + \delta\Phi$ (m is an integer) is the phase accumulated by the light beam in a single to-and-back passage along the length of the arm. For a large effective mean number of passages, $N_{\text{eff}} \gg 1$, and for sufficiently small deviations in the accumulated phase, $N_{\text{eff}} \cdot \delta\Phi \ll 1$, the sum in Eq. (2) can be written as:

$$\sum_{n=1}^{\infty} \exp[-n(\kappa - i\Phi)] \simeq N_{\text{eff}} \exp(iN_{\text{eff}} \cdot \delta\Phi), \quad (3)$$

from which it is evident that the effects of small variations in the accumulated phase are enhanced by the factor N_{eff} .

Variation of the electromagnetic fine-structure constant and particle masses. — Variation of α and particle masses alters the accumulated phase through alteration of ω and $L \sim Na_B$. There are four main classes of experimental configurations to consider, depending on whether the frequency of light inside an interferometer is determined by a specific atomic transition or by the length of a resonator, and whether the interferometer arm length is allowed to vary freely or its fluctuations are deliberately shielded (e.g. through the use of a multipendulum mirror system). We consider each of these configurations in turn.

Configuration A (atomic transition frequency, free arm length): The simplest case is when the frequency of light inside an interferometer is determined by an optical atomic transition frequency and the interferometer arm length is allowed to vary freely. A strontium clock – silicon cavity interferometer in its standard mode of operation falls into this category. In this case, the atomic transition wavelength and arm length are compared directly:

$$\Phi = \frac{\omega L}{c} \propto \left(\frac{e^2}{a_B \hbar}\right) \left(\frac{Na_B}{c}\right) = N\alpha, \quad (4)$$

where the optical atomic transition frequency ω is proportional to the atomic unit of frequency $e^2/a_B \hbar$. Variation of α thus gives rise to the following phase shift:

$$\delta\Phi \simeq \Phi \frac{\delta\alpha}{\alpha}. \quad (5)$$

We note that the effect of variation of α already appears at the non-relativistic level in Eq. (5), with the corresponding sensitivity coefficient $K_\alpha = 1$. For systems consisting of light elements, the relativistic corrections to this sensitivity coefficient are small and can be neglected. This is in stark contrast to optical clock comparison experiments, for which $K_\alpha = 0$ in the non-relativistic approximation and the contributions to K_α arise solely from relativistic corrections [37].

For a strontium clock – silicon cavity interferometer, which operates on the $^{87}\text{Sr } ^1S_0 - ^3P_0$ transition ($\lambda = 698$ nm) and for which the cavity length is $L = 0.21$ m [73], the phase shift in Eq. (5) for a single to-and-back passage of the light beam is:

$$\delta\Phi \simeq 3.8 \times 10^6 \frac{\delta\alpha}{\alpha}. \quad (6)$$

For comparison, in a large-scale gravitational-wave detector of length $L = 4$ km and operating on a typical atomic optical transition frequency, the phase shift for a single to-and-back passage of the light beam is:

$$\delta\Phi \sim 10^{11} \frac{\delta\alpha}{\alpha}. \quad (7)$$

As we have shown above, multiple reflections enhance the coefficients in Eqs. (6) and (7) by the effective mean number of passages N_{eff} . For large-scale interferometers, this enhancement factor is $N_{\text{eff}} \sim 10^2$. For a strontium clock – silicon cavity interferometer, this enhancement factor is considerably larger: $N_{\text{eff}} \sim 10^5$.

Another possible system in this category is the hydrogen maser – cryogenic sapphire oscillator system, for which changes in the measured phase have the following dependence on changes in the fundamental constants [64]:

$$\frac{\delta\Phi}{\Phi} \simeq 3 \frac{\delta\alpha}{\alpha} + \frac{\delta m_e}{m_e} - 0.1 \frac{\delta m_q}{m_q}, \quad (8)$$

where m_q is the light quark mass.

If one performs two simultaneous interferometry experiments with two different transition lines, using the same set of mirrors, then one may search for variations of the fundamental constants associated with changes in the atomic transition frequencies:

$$\delta X = \frac{c(\omega_A \delta \Phi_B - \omega_B \delta \Phi_A)}{L(\omega_A \frac{\partial \omega_B}{\partial X} - \omega_B \frac{\partial \omega_A}{\partial X})}. \quad (9)$$

In particular, note that shifts in the arm lengths (due to variation of the fundamental constants or undesired effects, such as seismic noise or tidal effects) cancel in Eq. (9).

Configuration B (atomic transition frequency, fixed arm length): If fluctuations in the arm length are deliberately shielded, e.g. through the use of a multiple-pendulum mirror system, but ω is still determined by an atomic transition frequency, then changes in the measured phase $\Phi \propto \omega/c \propto m_e e^4 / \hbar^3 c = (m_e c / \hbar) \cdot (e^2 / \hbar c)^2$ have the following dependence on changes in the fundamental constants:

$$\frac{\delta \Phi}{\Phi} \simeq \frac{\delta m_e}{m_e} + 2 \frac{\delta \alpha}{\alpha}. \quad (10)$$

Configuration C (resonator-determined wavelength, free arm length): When a laser is locked to a resonator mode determined by the length of the resonator, ω is determined by the length of the resonator, which changes if the fundamental constants change. In the non-relativistic limit, the wavelength and arm length (as well as the size of Earth) have the same dependence on the Bohr radius, and so there are no observable effects if changes of the fundamental constants are slow (adiabatic) and if the interferometer arm length is allowed to vary freely. Indeed, this may be viewed as a simple change in the measurement units. Transient effects due to the passage of topological defects may still produce effects, since changes in ω and L may occur at different times.

The sensitivity of laser interferometry to non-transient effects is determined by relativistic corrections, which we estimate as follows. The size of an atom R is determined by the classical turning point of an external atomic electron. Assuming that the centrifugal term $\sim 1/R^2$ is small at large distances, we obtain $(Z_i + 1)e^2/R = -E$, where E is the energy of the external electron and Z_i is the net charge of the atomic species (for a neutral atom, $Z_i = 0$). This gives the relation: $\delta R/R = \delta(E/e^2)/|E/e^2|$. The single-particle relativistic correction to the energy in a many-electron atomic species is given by [37]:

$$\Delta_n \simeq E_n \frac{(Z\alpha)^2}{\nu(j+1/2)}, \quad (11)$$

where $E_n = -m_e e^4 (Z_i + 1)^2 / 2\hbar^2 \nu^2$ is the energy of the external atomic electron, j is its angular momentum, Z is the nuclear charge, and $\nu \sim 1$ is the effective principal quantum number. Variation of α thus gives rise to the

following phase shift:

$$\frac{\delta \Phi}{\Phi} \simeq 2\alpha^2 \left[\frac{Z_{\text{res}}^2}{\nu_{\text{res}}(j_{\text{res}} + 1/2)} - \frac{Z_{\text{arm}}^2}{\nu_{\text{arm}}(j_{\text{arm}} + 1/2)} \right] \frac{\delta \alpha}{\alpha}. \quad (12)$$

Note that the sensitivity coefficient depends particularly strongly on the factor Z^2 . $|K_\alpha| \ll 1$ for light atoms and may be of the order of unity in heavy atoms.

Configuration D (resonator-determined wavelength, fixed arm length): If fluctuations in the arm length are deliberately shielded and ω is determined by the length of the resonator, then changes in the measured phase $\Phi \propto 1/\lambda \propto 1/a_B$ have the following dependence on changes in the fundamental constants:

$$\frac{\delta \Phi}{\Phi} \simeq \frac{\delta m_e}{m_e} + \frac{\delta \alpha}{\alpha}. \quad (13)$$

A large-scale gravitational wave detector (such as LIGO, Virgo, GEO600 or TAMA300) in its standard mode of operation falls into this category.

Non-zero photon mass. — A non-zero photon mass alters the accumulated phase through alteration of ω , $L = NR$ (where R is the atomic radius) and c . In particular, if a non-zero photon mass is generated due to the interaction of photons with slowly moving dark matter ($v_{\text{DM}} \ll 1$), then the energy and momentum of the photons are approximately conserved and the photon speed changes according to:

$$\delta c \simeq -\frac{m_\gamma^2}{2\omega^2}. \quad (14)$$

The effects of a non-zero photon mass in atoms are more subtle. The potential of an atomic electron changes from Coulomb to Yukawa-type:

$$V_{\text{Coulomb}}(r) = \sum_i \frac{e^2}{|\mathbf{r} - \mathbf{r}_i|} - \frac{Ze^2}{r}, \quad (15)$$

$$\Rightarrow V_{\text{Yukawa}}(r) = \sum_i \frac{e^{-m_\gamma |\mathbf{r} - \mathbf{r}_i|} e^2}{|\mathbf{r} - \mathbf{r}_i|} - \frac{e^{-m_\gamma r} Ze^2}{r}, \quad (16)$$

where the sum runs over all remaining atomic electrons. For $m_\gamma r \ll 1$, the leading term of the corresponding perturbation reads (we omit the constant terms, which do not alter the atomic transition frequencies and wavefunctions):

$$\delta V(r) = \frac{e^2 m_\gamma^2}{2} \left[\sum_i |\mathbf{r} - \mathbf{r}_i| - Zr \right], \quad (17)$$

which for a neutral atom takes the asymptotic forms:

$$\delta V(r) \simeq \begin{cases} -Ze^2 m_\gamma^2 r/2 & \text{when } r \ll a_B/Z^{1/3}, \\ -e^2 m_\gamma^2 r/2 & \text{when } r \gg a_B/Z^{1/3}. \end{cases} \quad (18)$$

In the semiclassical approximation, it is straightforward to confirm that the dominant contribution to the expectation value of the operator (17) comes from large distances, $r \gg a_B/Z^{1/3}$, where the external electron sees an

effective charge of $Z_{\text{eff}} = 1$. Therefore, the shift in an atomic energy level A is simply:

$$\delta E_A \simeq -\frac{e^2 m_\gamma^2 R_A}{2}, \quad (19)$$

where $R_A = \langle A|r|A \rangle$ is the expectation value of the radius operator for state A . Typically, $R_A \sim$ several a_B . Assuming that the perturbation (17) is adiabatic and that the dominant contribution to the matrix elements $\langle n|\delta V|A \rangle$ comes from large distances, application of time-independent perturbation theory gives the following shift in the size of the atomic orbit for state A :

$$\delta R_A \simeq -m_\gamma^2 \sum_{n \neq A} \frac{\langle A|er|n \rangle \langle n|er|A \rangle}{E_A^{(0)} - E_n^{(0)}} \sim m_\gamma^2 \alpha_A, \quad (20)$$

where α_A is the static dipole polarisability of state A . Static dipole polarisabilities for the electronic ground states of neutral atoms range from $4.5 a_B^3$ in hydrogen to $400 a_B^3$ in caesium [74].

Configuration A (atomic transition frequency, free arm length): If ω is determined by an atomic transition frequency and the interferometer arm length is allowed to vary freely, then a non-zero photon mass produces the following changes in the measured phase $\Phi = \omega L/c$:

$$\frac{\delta \Phi}{\Phi} \simeq \frac{e^2 m_\gamma^2 (R_f - R_i)}{2\omega} + \frac{m_\gamma^2 \alpha_{\text{arm}}}{R_{\text{arm}}} + \frac{m_\gamma^2}{2\omega^2} \simeq \frac{m_\gamma^2}{2\omega^2}, \quad (21)$$

where $R_f - R_i = \langle f|r|f \rangle - \langle i|r|i \rangle$ is the difference in the orbital size between the final and initial states involved in the radiative atomic transition. The three separate contributions in Eq. (21) scale roughly in the ratio $\alpha^2 : \alpha^2 : 1$, respectively, meaning that the contribution from the change in the photon speed dominates.

Configuration B (atomic transition frequency, fixed arm length): If fluctuations in the arm length are deliberately shielded, but ω is still determined by an atomic transition frequency, then a non-zero photon mass produces the following changes in the measured phase $\Phi \propto \omega/c$:

$$\frac{\delta \Phi}{\Phi} \simeq \frac{e^2 m_\gamma^2 (R_f - R_i)}{2\omega} + \frac{m_\gamma^2}{2\omega^2} \simeq \frac{m_\gamma^2}{2\omega^2}, \quad (22)$$

where we again note that the contribution from the change in the photon speed dominates.

Configuration C (resonator-determined wavelength, free arm length): If ω is determined by the length of the resonator and the interferometer arm length is allowed to vary freely, then a non-zero photon mass produces the following changes in the measured phase $\Phi = 2\pi L/\lambda$:

$$\frac{\delta \Phi}{\Phi} \sim m_\gamma^2 \left(\frac{\alpha_{\text{arm}}}{R_{\text{arm}}} - \frac{\alpha_{\text{res}}}{R_{\text{res}}} \right). \quad (23)$$

The phase shift in Eq. (23) is suppressed by the factor $\sim \alpha^2$ in the static limit (compare with Eqs. (21) and (22)

above). However, for time-dependent effects, the phase shift can be significantly larger (see the examples below).

Configuration D (resonator-determined wavelength, fixed arm length): If fluctuations in the arm length are deliberately shielded and ω is determined by the length of the resonator, then a non-zero photon mass produces the following changes in the measured phase $\Phi \propto 1/\lambda$:

$$\frac{\delta \Phi}{\Phi} \sim -m_\gamma^2 \frac{\alpha_{\text{res}}}{R_{\text{res}}}. \quad (24)$$

Similarly to Eq. (23), the phase shift in Eq. (24) is also suppressed by the factor $\sim \alpha^2$ in the static limit. However, we again note that the phase shift can be significantly larger for time-dependent effects.

Specific examples. — *Oscillating classical dark matter (effects of spatial coherence).* — Oscillating classical dark matter exhibits not only temporal coherence [31], but also spatial coherence, with a coherence length given by: $l_{\text{coh}} \sim 1/m_\phi v_{\text{vir}} \sim 10^3/m_\phi$, where m_ϕ is the dark matter particle mass, and a virial (root-mean-square) speed of $v_{\text{vir}} \sim 10^{-3}$ is typical in our local galactic neighbourhood. Our Solar System travels through the Milky Way (and hence relative to galactic dark matter) at a comparable speed (v) $\sim v_{\text{vir}} \sim 10^{-3}$. An oscillating scalar dark matter field takes the form:

$$\phi(\mathbf{r}, t) \simeq \phi_0 \cos(m_\phi t - m_\phi \langle \mathbf{v} \rangle \cdot \mathbf{r}), \quad (25)$$

meaning that measurements performed on length scales $l \lesssim 1/m_\phi v_{\text{vir}}$ are sensitive to dark matter-induced effects that arise from differences in the spatial phase term $m_\phi \langle \mathbf{v} \rangle \cdot \mathbf{r}$ at two or more points.

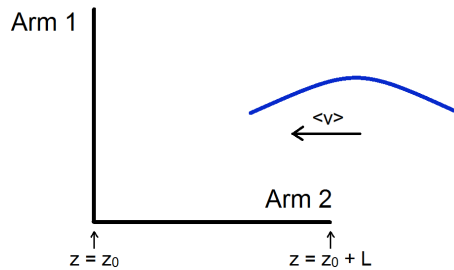


FIG. 1. (Color online) Passage of dark matter directly onto an arm of a gravitational-wave detector ($L_1 = L_2 = L$).

As a specific example, we consider measurements performed using a large-scale gravitational-wave detector with equal arm lengths that are deliberately shielded from fluctuations, $L_1 = L_2 = L = \text{constant}$, and with the emitted photon wavelength determined by the length of the resonator. Since we are considering slowly moving dark matter ($v_{\text{DM}} \ll 1$), changes in the wavelength of the travelling photon are related to changes in c by: $\delta\lambda/\lambda \simeq \delta c \simeq -[m_\gamma(\mathbf{r}, t)]^2/2\omega^2$, where the interaction between the photon field and ϕ^2 may be interpreted as the varying photon mass: $[m_\gamma(\mathbf{r}, t)]^2 = (m_\gamma)_{\text{max}}^2 \cos^2(m_\phi t - m_\phi \langle \mathbf{v} \rangle \cdot \mathbf{r})$. For the simplest case

when the dark matter is incident directly onto one of the detector arms as shown in Fig. 1, the shift in the accumulated phase difference between the two arms is given by:

$$\delta(\Phi_1 - \Phi_2) = \frac{2\pi}{\lambda} \int_{z_0}^{z_0+L} \left[\frac{\delta\lambda(z)}{\lambda} - \frac{\delta\lambda(z_0)}{\lambda} \right] dz, \quad (26)$$

and to leading order we find:

$$\frac{\delta(\Phi_1 - \Phi_2)}{\Phi} \simeq \frac{(m_\gamma)_{\max}^2 m_\phi \langle v \rangle L}{4\omega^2} \sin(2m_\phi t + 2m_\phi \langle v \rangle z_0). \quad (27)$$

The shift in the accumulated phase difference between the two arms in Eq. (27) is suppressed by the factor $m_\phi \langle v \rangle L < 1$.

Topological defect dark matter. — Topological defect dark matter is intrinsically coherent, both temporally and spatially. As a specific example, we again consider measurements performed using a large-scale gravitational-wave detector with equal arm lengths that are deliberately shielded from fluctuations and with the emitted photon wavelength determined by the length of the resonator. For the case of a 2D domain wall with a Gaussian cross-sectional profile of root-mean-square width $d \sim 1/m_\phi$ and which travels slowly ($v_{\text{TD}} \ll 1$) in the geometry shown in Fig. 1, the interaction between the photon field and ϕ^2 may be interpreted as the varying photon mass: $[m_\gamma(z, t)]^2 = (m_\gamma)_{\max}^2 \exp[-(z + vt)^2/d^2]$. Calculating the shift in the accumulated phase difference between the two arms, Eq. (26), we find to leading order:

$$\begin{aligned} \frac{\delta(\Phi_1 - \Phi_2)}{\Phi} \simeq & \frac{(m_\gamma)_{\max}^2}{2\omega^2} \left\{ \exp \left[-\frac{(z_0 + tv)^2}{2d^2} \right] \right. \\ & \left. - \sqrt{\frac{\pi}{2}} \cdot \frac{d}{L} \left[\operatorname{erf} \left(\frac{L + tv + z_0}{\sqrt{2}d} \right) - \operatorname{erf} \left(\frac{tv + z_0}{\sqrt{2}d} \right) \right] \right\}, \end{aligned} \quad (28)$$

where erf is the standard error function. The shift in the accumulated phase difference between the two arms in Eq. (28) is largest for $d \sim L$. For $d \gg L$, the phase shift in (28) is suppressed by the factor $L/d \ll 1$. In the case

when $d \ll L$, the phase shift in (28) is suppressed by the factor $d/L \ll 1$ when the topological defect envelops arm 2 but remains far away from arm 1; however, at the times when the topological defect envelops arm 1, there is no such suppression.

Conclusions. — We have outlined new laser interferometer measurements to search for variation of the electromagnetic fine-structure constant α and particle masses (including a non-zero photon mass). We have proposed a strontium optical lattice clock – silicon single-crystal cavity interferometer as a novel small-scale platform for these new measurements. We have shown that multiple passages of a light beam inside an interferometer enhance the effects due to variation of the fundamental constants by the mean number of passages ($N_{\text{eff}} \sim 10^2$ for a large-scale gravitational-wave detector, such as LIGO, Virgo, GEO600 or TAMA300, while $N_{\text{eff}} \sim 10^5$ for a strontium clock – silicon cavity interferometer). Our proposed laser interferometer measurements may be implemented as an extremely precise tool in the direct detection of scalar dark matter. For oscillating classical scalar dark matter, a single interferometer is sufficient in principle, while for topological defects, a global network of interferometers is required. The current best sensitivities to length fluctuations are at the fractional level $\sim 10^{-22} - 10^{-23}$ in the frequency range $\sim 60 - 2000$ Hz for a large-scale gravitational-wave detector [75] and at the fractional level $\sim 10^{-16}$ in the frequency range $\sim 0.1 - 10$ Hz for a silicon-based cavity [73].

Acknowledgements. — We are very grateful to Jun Ye and Fritz Riehle for suggesting the strontium clock – silicon cavity interferometer as a suitable small-scale platform for our newly proposed measurements, and for important discussions. We would like to thank Bruce Allen, Dmitry Budker, Federico Ferrini, Hartmut Grote, Sergey Klimenko, Giovanni Losurdo, Guenakh Mitselmakher and Surjeet Rajendran for helpful discussions. This work was supported by the Australian Research Council. V. V. F. is grateful to the Mainz Institute for Theoretical Physics (MITP) for its hospitality and support.

-
- [1] Bertone, G. (Ed.) *Particle Dark Matter: Observations, Models and Searches*. (Cambridge University Press, Cambridge, 2010).
- [2] R. Agnese *et al.* (SuperCDMS Collaboration), Search for Low-Mass Weakly Interacting Massive Particles with SuperCDMS. *Phys. Rev. Lett.* **112**, 241302 (2014).
- [3] C. E. Aalseth *et al.* (CoGeNT Collaboration), Results from a Search for Light-Mass Dark Matter with a P-type Point Contact Germanium Detector. *Phys. Rev. Lett.* **106**, 131301 (2011).
- [4] G. Angloher *et al.* (CRESST Collaboration), Results on low mass WIMPs using an upgraded CRESST-II detector. *Eur. Phys. J. C* **74**, 3184 (2014).
- [5] R. Bernabei *et al.* (DAMA/LIBRA Collaboration), First results from DAMA/LIBRA and the combined results with DAMA/NaI. *Eur. Phys. J. C* **56**, 333 (2008).
- [6] D. S. Akerib *et al.* (LUX Collaboration), The Large Underground Xenon (LUX) experiment. *NIMPA* **704**, 111 (2013).
- [7] E. Aprile *et al.* (XENON100 Collaboration), Limits on Spin-Dependent WIMP-Nucleon Cross Sections from 225 Live Days of XENON100 Data. *Phys. Rev. Lett.* **111**, 021301 (2013).
- [8] S. J. Asztalos, SQUID-Based Microwave Cavity Search for Dark-Matter Axions. *Phys. Rev. Lett.* **104**, 041301 (2010).

- [9] P. W. Graham, S. Rajendran, Axion dark matter detection with cold molecules. *Phys. Rev. D* **84**, 055013 (2011).
- [10] O. K. Baker, M. Betz, F. Caspers, J. Jaeckel, A. Lindner, A. Ringwald, Y. Semertzidis, P. Sikivie, K. Zioutas, Prospects for searching axionlike particle dark matter with dipole, toroidal, and wiggler magnets. *Phys. Rev. D* **85**, 035018 (2012).
- [11] M. Pospelov, S. Pustelny, M. P. Ledbetter, D. F. J. Kimball, W. Gawlik, D. Budker, Detecting Domain Walls of Axionlike Models Using Terrestrial Experiments. *Phys. Rev. Lett.* **110**, 021803 (2013).
- [12] A. Khmelnitsky, V. Rubakov, Pulsar timing signal from ultralight scalar dark matter. *JCAP* **02**, 019 (2014).
- [13] C. Beck, Possible Resonance Effect of Axionic Dark Matter in Josephson Junctions. *Phys. Rev. Lett.* **111**, 231801 (2013).
- [14] P. Sikivie, N. Sullivan, D. B. Tanner, Proposal for Axion Dark Matter Detection Using an LC Circuit. *Phys. Rev. Lett.* **112**, 131301 (2014).
- [15] Y. V. Stadnik, V. V. Flambaum, Axion-induced effects in atoms, molecules, and nuclei: Parity nonconservation, anapole moments, electric dipole moments, and spin-gravity and spin-axion momentum couplings. *Phys. Rev. D* **89**, 043522 (2014).
- [16] D. Budker, P. W. Graham, M. Ledbetter, S. Rajendran, A. O. Sushkov, Proposal for a Cosmic Axion Spin Precession Experiment (CASPER). *Phys. Rev. X* **4**, 021030 (2014).
- [17] B. M. Roberts, Y. V. Stadnik, V. A. Dzuba, V. V. Flambaum, N. Leefler, D. Budker. Limiting P-Odd Interactions of Cosmic Fields with Electrons, Protons, and Neutrons. *Phys. Rev. Lett.* **113**, 081601 (2014).
- [18] N. K. Porayko, K. A. Postnov, Constraints on ultralight scalar dark matter from pulsar timing. *Phys. Rev. D* **90**, 062008 (2014).
- [19] P. Sikivie, Axion Dark Matter Detection using Atomic Transitions. *Phys. Rev. Lett.* **113**, 201301 (2014).
- [20] A. Derevianko, M. Pospelov, Hunting for topological dark matter with atomic clocks. *Nat. Phys.* **10**, 933 (2014).
- [21] Y. V. Stadnik, V. V. Flambaum, Searching for Topological Defect Dark Matter via Nongravitational Signatures. *Phys. Rev. Lett.* **113**, 151301 (2014).
- [22] B. M. Roberts, Y. V. Stadnik, V. A. Dzuba, V. V. Flambaum, N. Leefler, D. Budker. Parity-violating interactions of cosmic fields with atoms, molecules, and nuclei: Concepts and calculations for laboratory searches and extracting limits. *Phys. Rev. D* **90**, 096005 (2014).
- [23] A. Arvanitaki, J. Huang, K. Van Tilburg, Searching for dilaton dark matter with atomic clocks. *Phys. Rev. D* **91**, 015015 (2015).
- [24] Y. V. Stadnik, V. V. Flambaum, Searching for Dark Matter and Variation of Fundamental Constants with Laser and Maser Interferometry. *Phys. Rev. Lett.* **114**, 161301 (2015).
- [25] C. Beck, Axion mass estimates from resonant Josephson junctions. *Phys. Dark Univ.* **7**, 6 (2015).
- [26] V. A. Popov, Resonant SQUID-based detection of Dark Matter Axion using rectangle cavities. *Space, Time and Fundamental Interactions* **4**, 39 (2015).
- [27] K. Van Tilburg, N. Leefler, L. Bougas, D. Budker, Search for ultralight scalar dark matter with atomic spectroscopy. *Phys. Rev. Lett.* **115**, 011802 (2015).
- [28] Y. V. Stadnik, V. V. Flambaum, Can dark matter induce cosmological evolution of the fundamental constants of Nature? *Phys. Rev. Lett.* (In press); arXiv:1503.08540.
- [29] P. A. M. Dirac, The Cosmological Constants. *Nature (London)* **139**, 323 (1937).
- [30] J.-P. Uzan, Varying Constants, Gravitation and Cosmology. *Living Rev. Relativity* **14**, 2 (2011).
- [31] Oscillating classical spin-0 dark matter can be readily produced in the early Universe through non-thermal production mechanisms (e.g. through vacuum decay [32–34]), with a very large coherence time. During galactic structure formation, gravitational interactions between dark matter and ordinary matter result in the virialisation of the dark matter particles, which gives a finite (but large) coherence time: $\tau_{\text{coh}} \sim 1/m_\phi v_{\text{vir}}^2 \sim 10^6/m_\phi$ (i.e. $\Delta\omega/\omega \sim 10^{-6}$), where m_ϕ is the dark matter particle mass, and a virial (root-mean-square) speed of $v_{\text{vir}} \sim 10^{-3}$ is typical in our local galactic neighbourhood.
- [32] J. Preskill, M. B. Wise, F. Wilczek, Cosmology of the Invisible Axion. *Phys. Lett. B* **120**, 127 (1983).
- [33] L. F. Abbott, P. Sikivie, A cosmological bound on the invisible axion. *Phys. Lett. B* **120**, 133 (1983).
- [34] M. Dine, W. Fischler, The not-so-harmless axion. *Phys. Lett. B* **120**, 137 (1983).
- [35] A. Vilenkin, Cosmic strings and domain walls. *Phys. Rep.* **121**, 263 (1985).
- [36] J. D. Prestage, R. L. Tjoelker, L. Maleki, Atomic Clocks and Variations of the Fine Structure Constant. *Phys. Rev. Lett.* **74**, 3511 (1995).
- [37] V. A. Dzuba, V. V. Flambaum, J. K. Webb, Space-Time Variation of Physical Constants and Relativistic Corrections in Atoms. *Phys. Rev. Lett.* **82**, 888 (1999).
- [38] M. Fischer *et al.*, New Limits on the Drift of Fundamental Constants from Laboratory Measurements. *Phys. Rev. Lett.* **92**, 230802 (2004).
- [39] V. V. Flambaum, A. F. Tedesco, Dependence of nuclear magnetic moments on quark masses and limits on temporal variation of fundamental constants from atomic clock experiments. *Phys. Rev. C* **73**, 055501 (2006).
- [40] T. Rosenband *et al.*, Frequency Ratio of Al^+ and Hg^+ Single-Ion Optical Clocks; Metrology at the 17th Decimal Place. *Science* **319**, 1808 (2008).
- [41] N. Leefler, C. T. M. Weber, A. Cingoz, J. R. Torgerson, D. Budker, New limits on variation of the fine-structure constant using atomic dysprosium. *Phys. Rev. Lett.* **111**, 060801 (2013).
- [42] R. M. Godun *et al.*, Frequency Ratio of Two Optical Clock Transitions in $^{171}\text{Yb}^+$ and Constraints on the Time Variation of Fundamental Constants. *Phys. Rev. Lett.* **113**, 210801 (2014).
- [43] N. Huntemann, B. Lipphardt, C. Tamm, V. Gerginov, S. Weyers, E. Peik, Improved Limit on a Temporal Variation of m_p/m_e from Comparisons of Yb^+ and Cs Atomic Clocks. *Phys. Rev. Lett.* **113**, 210802 (2014).
- [44] J. C. Berengut, V. A. Dzuba, V. V. Flambaum, Enhanced Laboratory Sensitivity to Variation of the Fine-Structure Constant using Highly Charged Ions. *Phys. Rev. Lett.* **105**, 120801 (2010).
- [45] J. C. Berengut, V. A. Dzuba, V. V. Flambaum, A. Ong, Electron-Hole Transitions in Multiply Charged Ions for Precision Laser Spectroscopy and Searching for Variations in α . *Phys. Rev. Lett.* **106**, 210802 (2011).
- [46] J. C. Berengut, V. A. Dzuba, V. V. Flambaum, A. Ong, Optical Transitions in Highly Charged Californium Ions

- with High Sensitivity to Variation of the Fine-Structure Constant. *Phys. Rev. Lett.* **109**, 070802 (2012).
- [47] A. Derevianko, V. A. Dzuba, V. V. Flambaum, Highly Charged Ions as a Basis of Optical Atomic Clockwork of Exceptional Accuracy. *Phys. Rev. Lett.* **109**, 180801 (2012).
- [48] M. S. Safronova, V. A. Dzuba, V. V. Flambaum, U. I. Safronova, S. G. Porsev, M. G. Kozlov, Highly Charged Ions for Atomic Clocks, Quantum Information, and Search for α variation. *Phys. Rev. Lett.* **113**, 030801 (2014).
- [49] A. Windberger *et al.*, Identification of the Predicted $5s-4f$ Level Crossing Optical Lines with Applications to Metrology and Searches for the Variation of Fundamental Constants. *Phys. Rev. Lett.* **114**, 150801 (2015).
- [50] S. Schiller, V. Korobov, Tests of time independence of the electron and nuclear masses with ultracold molecules. *Phys. Rev. A* **71**, 032505 (2005).
- [51] V. V. Flambaum, Enhanced effect of temporal variation of the fine-structure constant in diatomic molecules. *Phys. Rev. A* **73**, 034101 (2006).
- [52] E. R. Hudson, H. J. Lewandowski, B. C. Sawyer, J. Ye, Cold Molecule Spectroscopy for Constraining the Evolution of the Fine Structure Constant. *Phys. Rev. Lett.* **96**, 143004 (2006).
- [53] V. V. Flambaum, M. G. Kozlov, Enhanced Sensitivity to the Time Variation of the Fine-Structure Constant and m_p/m_e in Diatomic Molecules. *Phys. Rev. Lett.* **99**, 150801 (2007).
- [54] T. Zelevinsky, S. Kotochigova, J. Ye, Precision Test of Mass-Ratio Variations with Lattice-Confined Ultracold Molecules. *Phys. Rev. Lett.* **100**, 043201 (2008).
- [55] D. DeMille, S. Sainis, J. Sage, T. Bergeman, S. Kotochigova, E. Tiesinga, Enhanced Sensitivity to Variation of m_e/m_p in Molecular Spectra. *Phys. Rev. Lett.* **100**, 043202 (2008).
- [56] V. V. Flambaum, Enhanced Effect of Temporal Variation of the Fine Structure Constant and the Strong Interaction in ^{229}Th . *Phys. Rev. Lett.* **97**, 092502 (2006).
- [57] A. C. Hayes, J. L. Friar, Sensitivity of nuclear transition frequencies to temporal variation of the fine structure constant or the strong interaction. *Phys. Lett. B* **650**, 229 (2007).
- [58] X.-T. He, Z.-Z. Ren, Temporal variation of the fine structure constant and the strong interaction parameter in the ^{229}Th transition. *Nucl. Phys. A* **806**, 117 (2008).
- [59] V. V. Flambaum, R. B. Wiringa, Enhanced effect of quark mass variation in ^{229}Th and limits from Oklo data. *Phys. Rev. C* **79**, 034302 (2009).
- [60] J. C. Berengut, V. A. Dzuba, V. V. Flambaum, S. G. Porsev, Proposed Experimental Method to Determine α Sensitivity of Splitting between Ground and 7.6 eV Isomeric States in ^{229}Th . *Phys. Rev. Lett.* **102**, 210801 (2009).
- [61] E. Litvinova, H. Feldmeier, J. Dobaczewski, V. Flambaum, Nuclear structure of lowest ^{229}Th states and time-dependent fundamental constants. *Phys. Rev. C* **79**, 064303 (2009).
- [62] W. G. Rellergert, D. DeMille, R. R. Greco, M. P. Hehlen, J. R. Torgerson, E. R. Hudson, Constraining the Evolution of the Fundamental Constants with a Solid-State Optical Frequency Reference Based on the ^{229}Th Nucleus. *Phys. Rev. Lett.* **104**, 200802 (2010).
- [63] J. P. Turneaure, S. R. Stein, An Experimental Limit on the Time Variation of the Fine Structure Constant, in *Atomic Masses and Fundamental Constants 5* [Editors: J. H. Sanders, A. H. Wapstra], 636 – 642 (1976).
- [64] M. E. Tobar, P. Wolf, S. Bize, G. Santarelli, V. Flambaum, Testing Local Lorentz and Position Invariance and Variation of Fundamental Constants by searching the Derivative of the Comparison Frequency Between a Cryogenic Sapphire Oscillator and Hydrogen Maser. *Phys. Rev. D* **81**, 022003 (2010).
- [65] S. Schiller, C. Laemmerzahl, H. Mueller, C. Braxmaier, S. Herrmann, A. Peters, Experimental limits for low-frequency space-time fluctuations from ultrastable optical resonators. *Phys. Rev. D* **69**, 027504 (2004).
- [66] M. Nagel *et al.*, Direct Terrestrial Test of Lorentz Symmetry in Electrodynamics to 10^{-18} . *Nature Comm.* **6**, 8174 (2015).
- [67] G. M. Harry (for the LIGO Scientific Collaboration), Advanced LIGO: the next generation of gravitational wave detectors. *Class. Quantum Grav.* **27**, 084006 (2010).
- [68] T. Accadia *et al.* (Virgo Collaboration), Status of the Virgo project. *Class. Quantum Grav.* **28**, 114002 (2011).
- [69] H. Grote (for the LIGO Scientific Collaboration), The GEO 600 status. *Class. Quantum Grav.* **27**, 084003 (2010).
- [70] R. Takahashi *et al.* (TAMA300 Collaboration), Operational status of TAMA300 with the seismic attenuation system (SAS). *Class. Quantum Grav.* **25**, 114036 (2008).
- [71] P. Amaro-Seoane *et al.*, eLISA: Astrophysics and cosmology in the millihertz regime. arXiv:1201.3621.
- [72] A. Chou *et al.*, *The Fermilab Holometer: A program to measure Planck scale indeterminacy* (Fermilab publication, Chicago, 2009).
- [73] T. Kessler *et al.*, A sub-40-mHz-linewidth laser based on a silicon single-crystal optical cavity. *Nature Photonics* **6**, 687 (2012).
- [74] P. Schwerdtfeger, Table of experimental and calculated static dipole polarizabilities for the electronic ground states of the neutral elements (in atomic units), last updated 2014, ctcp.massey.ac.nz/Tablepol2014.pdf
- [75] Ligo Scientific Collaboration and Virgo Collaboration, Sensitivity Achieved by the LIGO and Virgo Gravitational Wave Detectors during LIGO's Sixth and Virgo's Second and Third Science Runs. arXiv:1203.2674.